

# On the resolution of multivectorial remanences

Yongjae Yu\*, David J. Dunlop, Özden Özdemir

*Geophysics, Department of Physics, University of Toronto, 60 St. George Street, Toronto, M5S 1A7, Canada*

Received 3 October 2002; received in revised form 10 December 2002; accepted 16 December 2002

## Abstract

Low-temperature demagnetization (LTD) promotes single-domain (SD)-like alternating field (AF) and thermal demagnetization properties of anhysteretic remanent magnetization (ARM) and thermoremanent magnetization (TRM), by eliminating low-coercivity or low-unblocking-temperature fractions of remanence. We have investigated the effectiveness of LTD in improving the independence of partial ARMs (pARMs). Independence of pARMs and of partial TRMs (pTRMs) is crucial because multivectorial directional analyses and paleointensity determinations are otherwise compromised. In normalized vector plots of AF demagnetization of orthogonal pARMs, LTD-treated samples showed universal improvement in the degree of independence. The greatest improvement was for synthetic SD and pseudo-single-domain magnetites and natural lake sediments. On the other hand, independence barely improved for synthetic multidomain magnetite, granites, and gabbros. In general, LTD provides a better resolution of superimposed vectors in multicomponent remanence. The direction of the original ARM (corresponding to primary NRM in nature) is perfectly recovered. However, the pARM (the overprint) is not perfectly resolved, especially for overprinting coercivities < 40 mT, where the deviation in inclination is 10° or more.

© 2003 Elsevier Science B.V. All rights reserved.

*Keywords:* low-temperature demagnetization; anhysteretic remanence; partial anhysteretic remanence; independence; multivectorial remanence

## 1. Introduction

In low-temperature demagnetization (LTD), rocks containing magnetite are cooled to below the Verwey transition  $T_v$  ( $\sim 120$  K) and warmed to room temperature in zero field. LTD is quite effective in eliminating remanence fractions of low coercivity or low unblocking temperature [1]. As a result, LTD has been applied as a pre-treatment

before alternating field (AF) or thermal demagnetization. Since LTD causes unpinning of domain walls with no risk of oxidation as in thermal demagnetization, it has been used in several studies to obtain better resolution of paleodirections [1–5]. It was also observed that LTD improves the isolation of archeomagnetic signals [6] and the linearity in paleointensity determination [2]. Dunlop et al. [3,4] and Warnock et al. [5] systematically applied LTD to better dissect multivectorial natural remanent magnetizations (NRMs) in remagnetized rocks.

Yu et al. [7] have shown that when anhysteretic remanent magnetization (ARM, simulating pri-

\* Corresponding author. Tel.: +1-905-828-5440;  
Fax: +1-905-828-3717.  
E-mail address: [yjyu@physics.utoronto.ca](mailto:yjyu@physics.utoronto.ca) (Y. Yu).

primary NRM produced in a field  $H_1$ ) is orthogonally overprinted by partial ARM (pARM, simulating remagnetization in  $H_2$ ), the intensity of  $H_2$  and the direction of  $H_1$  are well resolved but the intensity of  $H_1$  was underestimated in an Arai-type plot, sometimes severely, and the estimated direction of  $H_2$  was deflected toward the direction of  $H_1$  [7]. These results indicate violation of the pARM independence law, i.e., a pARM produced over an AF interval ( $\tilde{H}_2, \tilde{H}_1$ ) affects the intensity and direction of another pARM whose AF interval does not overlap ( $\tilde{H}_2, \tilde{H}_1$ ). Although ARM is an artificial replica of NRM, using ARM has its merits. First, ARM techniques require no heating so that alteration of minerals is prevented. Second, additivity, reciprocity, and independence of pARMs can be tested in simple, quick experiments [7–9]. In particular, the independence of pARMs [7] was tested unambiguously by using orthogonal superposition of one or more pARMs on ARM.

In this study, we are not mainly interested in physical properties of magnetites at low temperatures (see the review by Muxworthy and McClelland [10]). Instead, we turn our attention to practical questions that were previously ignored. The goal of this paper is to provide a quantitative answer to the question, ‘How much can LTD improve the directional resolution of remanence vectors in multicomponent NRM?’

## 2. Samples

Eight synthetic samples were prepared using magnetite powders whose mean grain sizes range from single domain (SD, 0.065  $\mu\text{m}$ ) to small multidomain (MD, 18.3  $\mu\text{m}$ ) [8]. Samples are 0.5% by volume dispersions of magnetite in a matrix of  $\text{CaF}_2$ . Cylindrical pellets 8.8 mm in diameter and 8.6 mm in height were pressed and then tightly wrapped with quartz wool inside quartz capsules. The capsules were sealed under vacuum and annealed for 3 h at 700°C to stabilize the magnetic properties.

Twenty-six natural samples were also studied: two andesites and one red scoria [11], 14 gabbros [12,13], three granites [14,15], and six freeze-dried

lake sediments [16] (Table 1). The natural samples selected have magnetic and paleomagnetic properties that are well documented. They were chosen from a much larger collection of several hundred cores on the basis of their low magnetic fabric anisotropy, their reproducible ARM and TRM intensities (for sediments, ARM only), and minimal viscous magnetic changes. Low fabric anisotropy is necessary to produce remanences along two or three orthogonal axes using orthogonal fields. The gabbros and lake sediments had yielded reliable paleointensities by the Thellier and pseudo-Thellier methods, respectively.

## 3. Low-temperature memory

### 3.1. Experimental procedures

After thermal demagnetization to 600°C (or AF demagnetization to 100 mT for sediments), ARM1 was imparted in an AF decaying from 100 mT with a steady field of  $H = 50 \mu\text{T}$  along  $z$  using a Molspin AF demagnetizer. AF demagnetization was carried out to 100 mT in 5 mT steps in two different ways: first, along  $\pm z$  (single-axis demagnetization); second, along  $\pm x$ ,  $\pm y$ , and  $\pm z$  in succession (three-axis demagnetization). The results were slightly ( $\sim 1\%$ ) different in intensity, but we used three-axis demagnetization as our routine technique because it more efficiently eliminates spurious transverse ( $x$ ,  $y$ ) components. A second ARM, ARM2, was produced and cycled to 77 K and back to 300 K in zero field. The memory of ARM2 after the LTD cycle was measured ( $R_{A1}$  = memory of ARM2/total ARM) and then stepwise AF demagnetized. LTD was carried out in a zero-field ( $< 28$  nT) shielded space. Samples were held for 1 h at 77 K in a small Dewar filled with liquid nitrogen.

After thermal demagnetization to 600°C (or AF demagnetization to 100 mT for sediments), ARM3 was generated and then stepwise thermal demagnetization was carried out every 50°C from 200°C to 500°C and every 10°C between 510°C and 580°C, using an MMTD furnace. Another ARM4 was produced and then LTD treated. The memory of ARM4 ( $R_{A2}$  = memory of

ARM4/total ARM) was then thermally demagnetized, completing two sets of AF and two sets of thermal demagnetizations on ARM with and without prior LTD. Throughout all heat treatments, temperatures were reproducible within  $\pm 2^\circ\text{C}$ . The residual field in the furnace during heatings and coolings was less than 150 nT.

Similarly, two sets of AF demagnetizations on TRM1, TRM memory ( $R_{T1}$  memory ratio from TRM2), saturation remanent magnetization (SIRM) SIRM1, and SIRM memory ( $R_{S1}$  from SIRM2) and two sets of thermal demagnetizations on TRM (TRM3), TRM memory ( $R_{T2}$  from TRM4), SIRM (SIRM3), and SIRM mem-

ory ( $R_{S2}$  from SIRM4) were performed. SIRM was produced in a 1 T field, using an SC-10 impulse magnetizer. TRM was generated in a steady field  $H = 50 \mu\text{T}$ .

### 3.2. Low-temperature memory

Although many factors such as stress, grain shape, and degree of stoichiometry affect LTD memory, the memories of TRM and SIRM have fairly well established grain-size variations [17,18]. ARM, TRM, and SIRM memory ratios are listed (Table 1). For the synthetic samples, the results are plotted as a function of grain size in Fig. 1.

Table 1  
Low-temperature memory

	$R_{A1}$ <sup>a</sup>	$R_{A2}$ <sup>b</sup>	$R_{T1}$ <sup>a</sup>	$R_{T2}$ <sup>b</sup>	$R_{S1}$ <sup>a</sup>	$R_{S2}$ <sup>b</sup>	$R_{S3}$ <sup>c</sup>
Synthetic samples							
0.065 $\mu\text{m}$	0.771	0.809	0.869	0.883	0.689	0.680	0.906
0.21 $\mu\text{m}$	0.746	0.754	0.880	0.859	0.633	0.673	0.895
0.44 $\mu\text{m}$	0.925	0.849	0.941	0.915	0.827	0.902	0.892
0.24 $\mu\text{m}$	0.808	0.730	0.855	0.880	0.626	0.642	0.993
0.34 $\mu\text{m}$	0.617	0.604	0.718	0.716	0.516	0.489	0.882
1.06 $\mu\text{m}$	0.544	0.579	0.619	0.656	0.369	0.391	0.771
16.86 $\mu\text{m}$	0.286	0.393	0.288	0.360	0.210	0.227	0.437
18.31 $\mu\text{m}$	0.305	0.278	0.258	0.288	0.203	0.229	0.446
Lake sediments							
288 B	0.865				0.690		0.798
456 B	0.852				0.745		0.819
578 B	0.824				0.728		0.821
885 B	0.792				0.628		0.748
954 B	0.805				0.639		0.784
1004 B	0.802				0.662		0.789
Igneous/volcanic samples							
An 1	0.929	0.914	0.947	0.933	0.765	0.774	0.785
An 3	0.913	0.916	0.900	0.906	0.768	0.760	0.886
Bu 5	0.368	0.398	0.441	0.410	0.327	0.369	
Bu 8	0.337	0.429	0.432	0.400	0.307	0.386	0.299
C 6	0.959	0.955	0.992	0.988	0.885	0.920	
C 12	0.944	0.933	0.994	0.998	0.897	0.911	
Km 3	0.861	0.881	0.959	0.956	0.892	0.846	0.744
S 50	0.438	0.466	0.507	0.501	0.440	0.334	
T 2	0.622	0.557	0.664	0.651	0.442	0.426	0.543
T 19	0.900	0.824	0.923	0.919	0.750	0.728	0.709

Results for 10 other gabbros (Section 2) are not listed. They are very similar to those listed.

<sup>a,b</sup> ARM and TRM used bias field  $H = 50 \mu\text{T}$ . SIRM was generated in an applied field of 1 T. All vacuum-sealed synthetic samples were annealed.

<sup>a</sup> Memory measurements on ARM ( $R_{A1}$ ), TRM ( $R_{T1}$ ), and SIRM ( $R_{S1}$ ) before AF demagnetization.

<sup>b</sup> Memory measurements on ARM ( $R_{A2}$ ), TRM ( $R_{T2}$ ), and SIRM ( $R_{S2}$ ) before thermal demagnetization.

<sup>c</sup> Room-temperature SIRM was generated in an applied field of 2 T. Memory was obtained after cooling to 10 K and then warming to 300 K, using an MPMS. For natural samples, small chips from the sister specimen were used. For synthetic samples, unannealed powders were used.

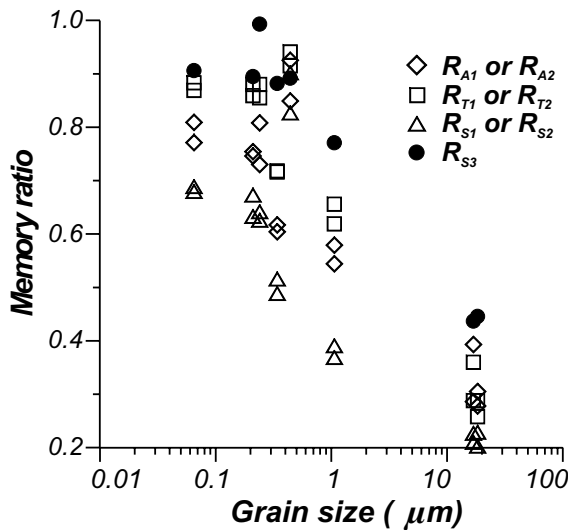


Fig. 1. Memory ratios of ARM, SIRM, and TRM of synthetic powders as a function of grain size. Memory ratios decrease as the grain size increases.

For annealed powders, regardless of the grain size, the general trend is  $R_T > R_A > R_S$  (Fig. 1 and Table 1). Unannealed powders can have considerably higher values of  $R_S$ , even larger than those of  $R_T$ , indicating that the remanence is strongly influenced by stress [17] (refer to Section 3.5 for the experimental sequence for  $R_{S3}$ ).

### 3.3. AF demagnetization

Fig. 2 illustrates AF demagnetization of ARM, SIRM, TRM, and their memories for three synthetic and three natural samples. The demagnetization curves after LTD were normalized to the corresponding pre-cooling values of ARM, SIRM, and TRM. For synthetic SD and pseudo-single-domain (PSD) magnetites, lake sediments, and gabbros, memories have more SD-like behavior compared to remanences without LTD, with an enhanced initial plateau at low AFs (Fig. 2a,b,d,e). The AF demagnetization of ARM, SIRM, and TRM of synthetic MD and granite samples shows a quasi-exponential decay

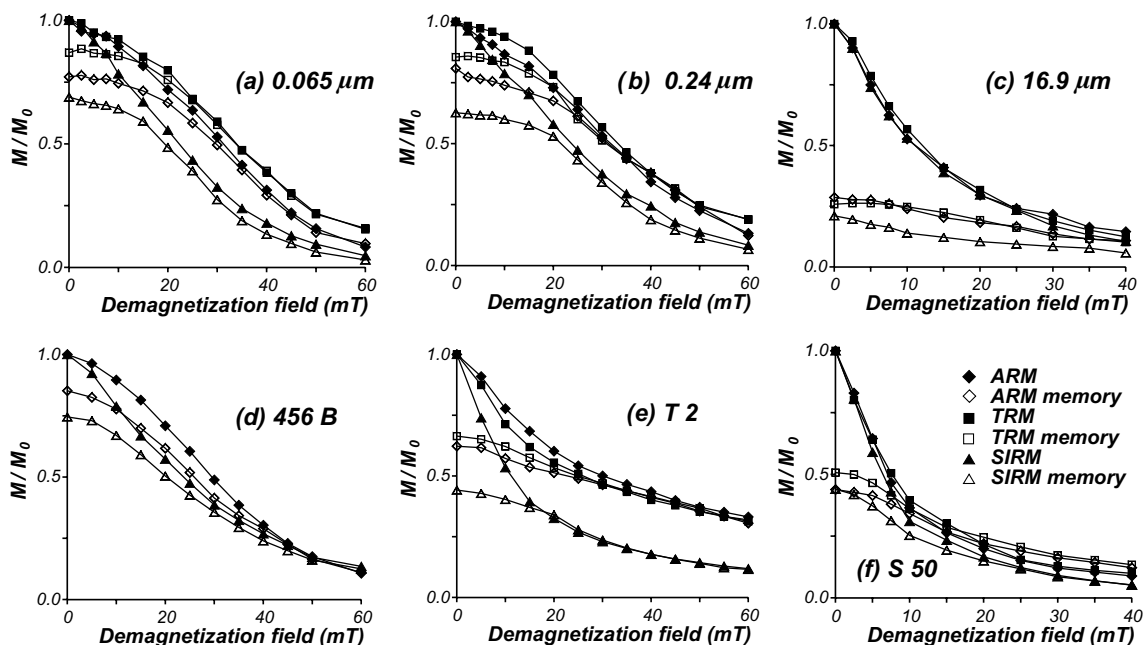


Fig. 2. AF demagnetization of ARM, SIRM, TRM, and their memories. For low-temperature memories, little remanence is lost at low AF. The LTD-treated and untreated curves converge at higher AFs.

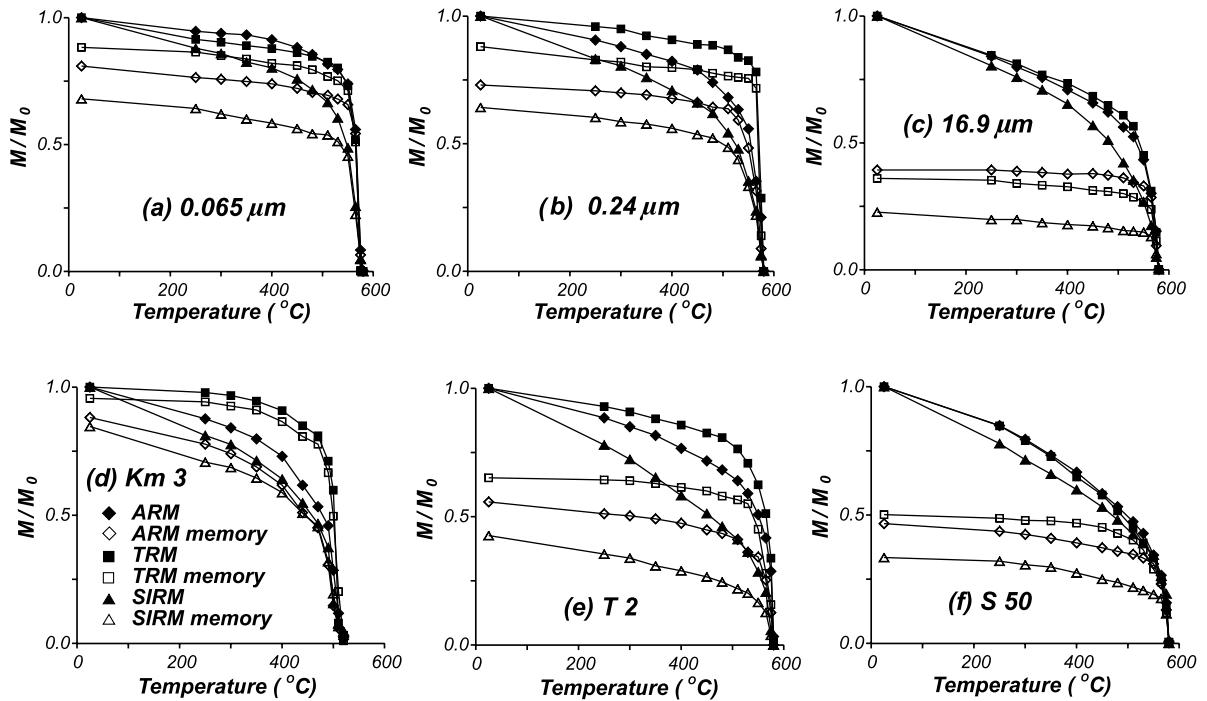


Fig. 3. Thermal demagnetization of ARM, SIRM, TRM, and their memories. For low-temperature memories, little remanence is lost at low temperatures. The LTD-treated and untreated curves converge at higher temperatures.

(Fig. 2c,f). Similar trends were reported for SD/PSD [19] and for MD grains [10,20].

### 3.4. Thermal demagnetization

Thermal demagnetization curves of ARM, TRM, and SIRM with and without prior LTD are strikingly different. Without LTD, thermal demagnetization curves of ARM and TRM for SD grains are nearly identical (Fig. 3a). For PSD grains, without LTD, the relative hardness of remanences is TRM > ARM > SIRM (Fig. 3b), a typical trend reported previously [21,22]. Similar trends are shown for natural samples in the PSD range (Fig. 3d,e). These distinct characteristics are less pronounced after LTD. For LTD-treated remanences, especially TRM, thermal demagnetization follows a flat plateau up to 500–540°C and then shows a sudden decrease of remanence above these temperatures (Fig. 3a,b,e). In other words, LTD makes remanences more SD-like by removing distributed unblocking temperatures < 500–540°C. However, the effect of LTD on titanomag-

netite ( $x \approx 0.1$ ) in sample Km 3 is different. LTD barely changes the unblocking temperature spectra (Fig. 3d).

For synthetic MD grains and granite containing MD magnetite, ~45–50% of ARM, TRM, and SIRM decay at a fairly steady rate up to 540°C (Fig. 3c,f). The remaining remanence shows rather an abrupt demagnetization in a narrow interval between 540°C and 580°C. After LTD treatment, memories became very stable against thermal demagnetization, so that almost no remanence was demagnetized below 540°C. Therefore, regardless of grain size and the types of initial remanences, LTD memories of magnetite are almost entirely composed of very high unblocking temperatures, > 500–540°C.

### 3.5. Isothermal remanence cooling and warming curves

Continuous measurement of isothermal remanence during zero-field cooling (300 K to 10 K) and warming (10 K to 300 K) is a means of de-

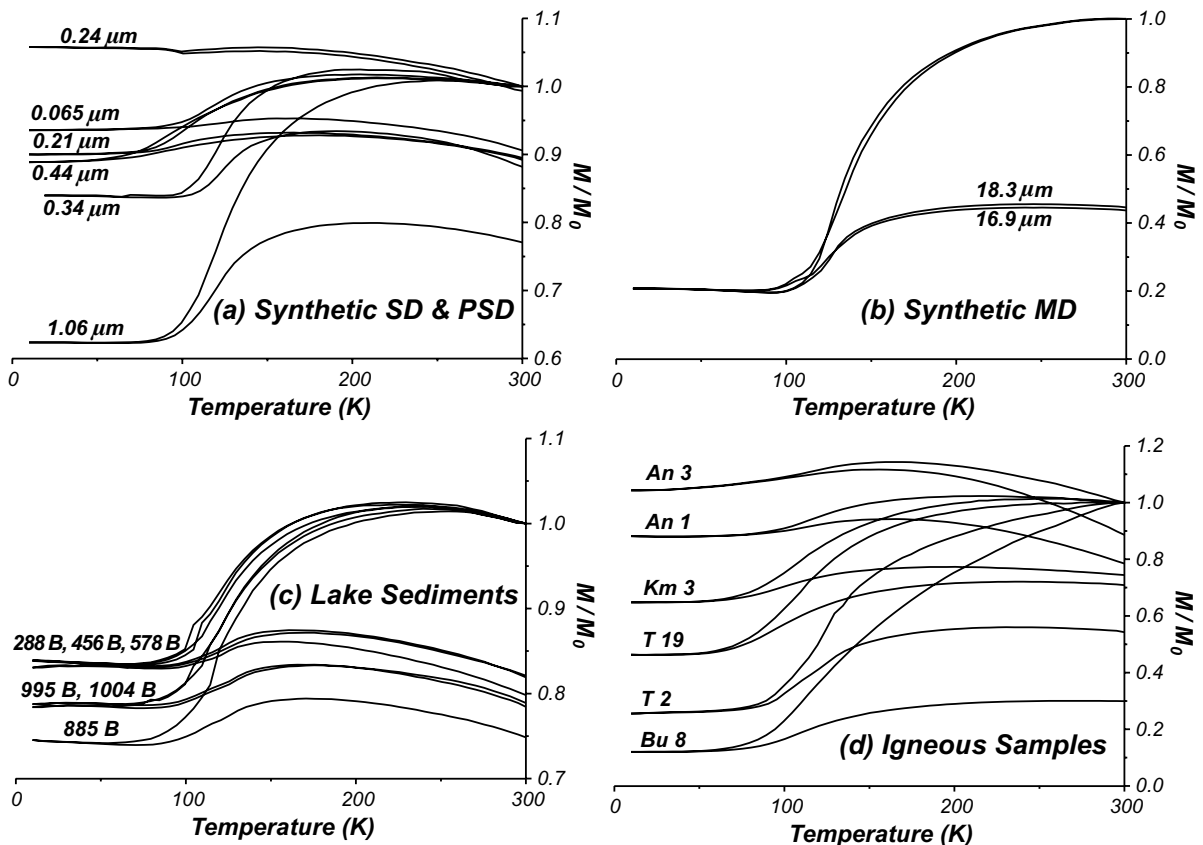


Fig. 4. Isothermal remanence cooling and warming curves. SIRM was produced in 2 T at 300 K. In general, remanence decreases during cooling but is partially recovered on warming through  $T_v$ .

termining average grain size of magnetite [23]. We produced room-temperature SIRM in an applied field of 2 T. Memory (ratio  $R_{S3}$ ) of this SIRM was obtained after cooling in zero field ( $< 0.5 \mu\text{T}$ ) to 10 K and then warming to 300 K, using a Quantum Design MPMS at the Institute for Rock Magnetism, University of Minnesota. For natural samples, we used small chips extracted from sister specimens. Unannealed powders were used for synthetic samples.

All the samples, regardless of their grain size and lithology, show reversible behavior at low temperatures (10 K to 70–90 K) but irreversible behavior with partial recovery of original remanence at higher temperature (70–90 K to 300 K) (Fig. 4). For synthetic samples, the remanence decrease  $\sim T_v$  during cooling and the remanence

increase at  $T_v$  during warming become more prominent as the average grain size increases (Fig. 4a,b). On the other hand, the recovery of initial remanence at 300 K, i.e., the SIRM memory, decreases with increasing grain size. For natural lake sediments, room-temperature SIRM cooling and warming curves mimic the results of synthetic PSD magnetites, implying average grain sizes of magnetite in the sediments of  $\sim 1 \mu\text{m}$  (Fig. 4c). Igneous samples show a wide variation, from MD-like (Bu 8) to SD-like (An 1 and Km 3) (Fig. 4d). One interesting and novel result is the increasing remanence during initial cooling from 300 K to near  $T_v$  in 0.24  $\mu\text{m}$  magnetite and An 3. This phenomenon probably results from mixed shape and crystalline anisotropies in SD grains [23].

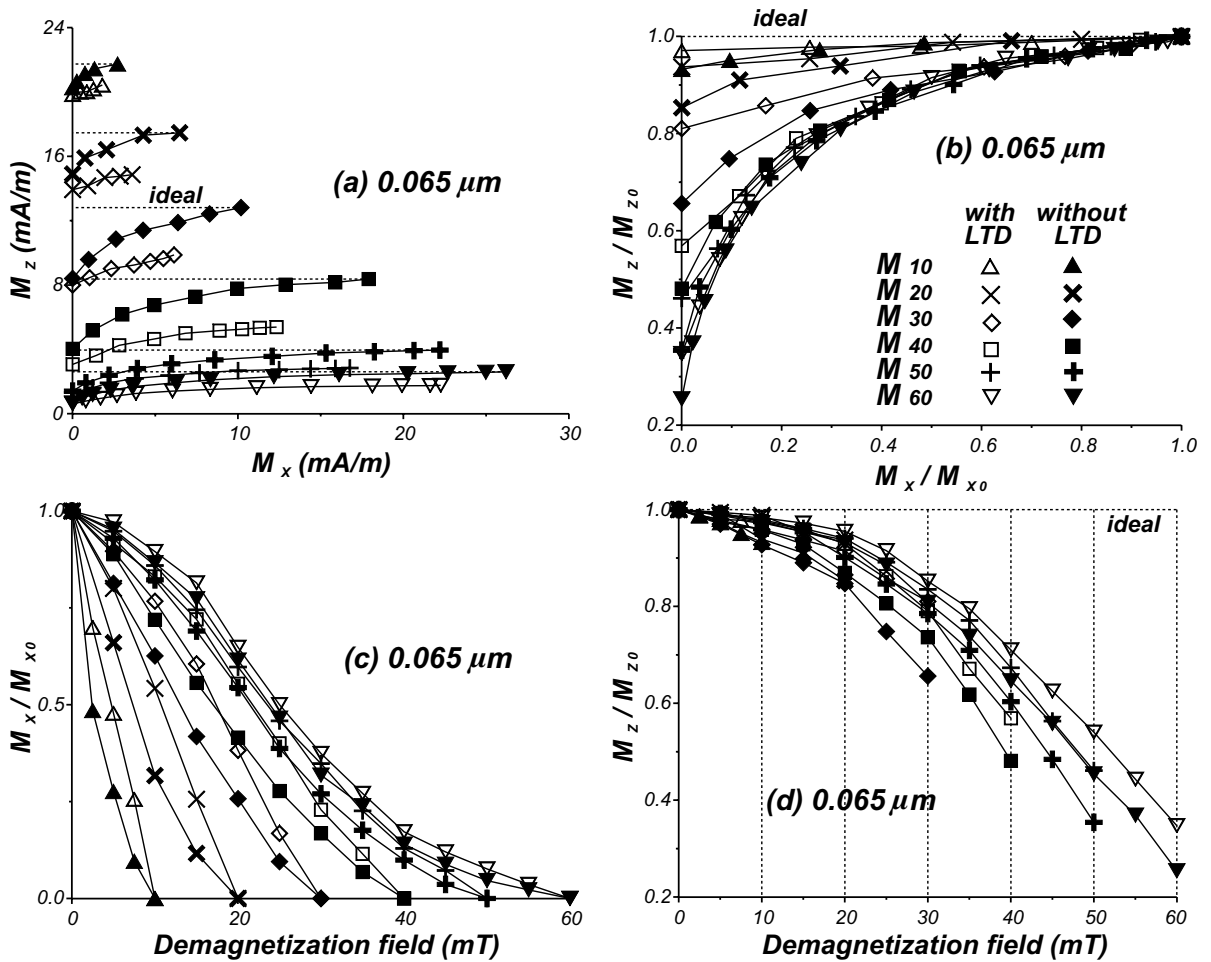


Fig. 5. AF demagnetization of  $ARM_z+pARM_x$  for the 0.065  $\mu m$  SD sample with and without LTD. (a) Vector plots. (b) Normalized vector plots. Decay curves for (c)  $x$  and (d)  $z$  components.

#### 4. Effect of LTD on pARM independence

##### 4.1. Experimental procedures

To examine the independence of pARMs, we first produced total  $ARM_z$  (100 mT, 0) along  $z$  in an AF decaying from 100 mT with a steady field of  $H=50 \mu T$ . Then  $ARM_z$  was partially overprinted by  $pARM_x(\tilde{H}_i,0)$  along  $x$  over the AF range  $\tilde{H}_i$  to 0. Six different orthogonal sums  $ARM_z+pARM_x(\tilde{H}_i,0)$  for  $\tilde{H}_i=10, 20, 30, 40, 50,$  and 60 mT yielded vector resultants  $M_{10}, M_{20}, M_{30}, M_{40}, M_{50},$  and  $M_{60}$ , respectively. Each of these remanences was AF demagnetized in 5 mT steps to 100 mT.  $M_{10}-M_{60}$  were then re-produced

and LTD was carried out before stepwise AF demagnetization.

In the ideal case, the total ARM aligns all coercivity fractions from 0 to 100 mT along  $z$ . The later remagnetization  $pARM_x(\tilde{H}_i,0)$  should redirect the coercivity fraction  $(\tilde{H}_i,0)$  along  $x$ , leaving the fraction (100 mT,  $\tilde{H}_i$ ) untouched. Therefore, during AF demagnetization from 0 to  $\tilde{H}_i$ , only  $M_x$  should decay while  $M_z$  should remain constant for ideal independence (dashed lines in Figs. 5, 6, and 7).

##### 4.2. Results

Typical examples are presented in the form of

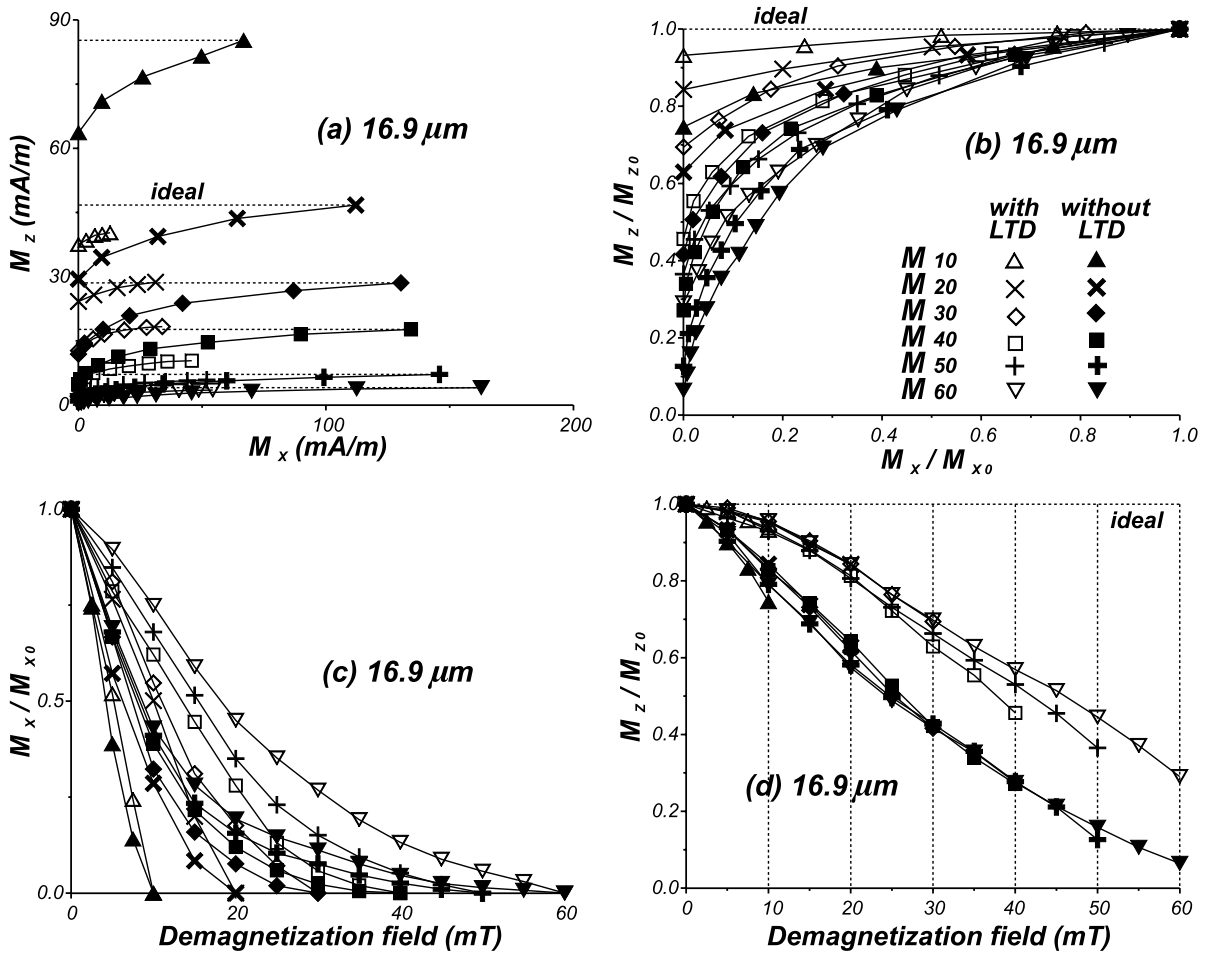


Fig. 6. AF demagnetization of ARM<sub>z</sub>+pARM<sub>x</sub> for the 16.9 μm MD sample with and without LTD. (a) Vector plots. (b) Normalized vector plots. Decay curves for (c) *x* and (d) *z* components.

orthogonal vector plots (Figs. 5a, 6a, 7a), normalized vector plots (Figs. 5b, 6b, 7b), and component decay curves for *M<sub>x</sub>* (Figs. 5c, 6c, 7c) and for *M<sub>z</sub>* (Figs. 5d, 6d, 7d). AF demagnetization results for  $\tilde{H} > \tilde{H}_i$  follow the vertical axis on vector plots and are not shown (Figs. 5a,b, 6a,b, 7a,b). Dashed lines (Figs. 5a,b,d, 6a,b,d, 7a,b,d) represent ideal independence.

In Fig. 5, SD magnetite (0.065 μm) shows distinctly different demagnetization behavior before and after LTD. The main effect of LTD on the softer pARM<sub>x</sub> ( $\tilde{H}_i, 0$ ) overprint (*M<sub>x</sub>* component) is to enhance the initial plateau at low AFs (Fig. 5c). Notice that all the overprint is erased by AF demagnetization to  $\tilde{H}_i$ .

For true independence, the harder overprinted ARM<sub>z</sub> (*M<sub>z</sub>* component) should remain constant up to  $\tilde{H}_i$  without showing any decay. This is illustrated in the ideal vector plots and *M<sub>z</sub>* curves of Fig. 5d. In reality, *M<sub>z</sub>* decayed to some extent below  $\tilde{H}_i$  even for SD grains. After LTD treatment, the independence of *M<sub>z</sub>* improved somewhat: less of *M<sub>z</sub>* demagnetized below  $\tilde{H}_i$ .

In vector projections, remanence demagnetization trajectories before LTD are more curved while after LTD the trajectories are more linear (Fig. 5a). Although a normalized vector plot has no practical application in directional analyses, it is of use in judging the improvement in independence since the value of the intercept *M<sub>z</sub>*/*M<sub>z0</sub>* rep-

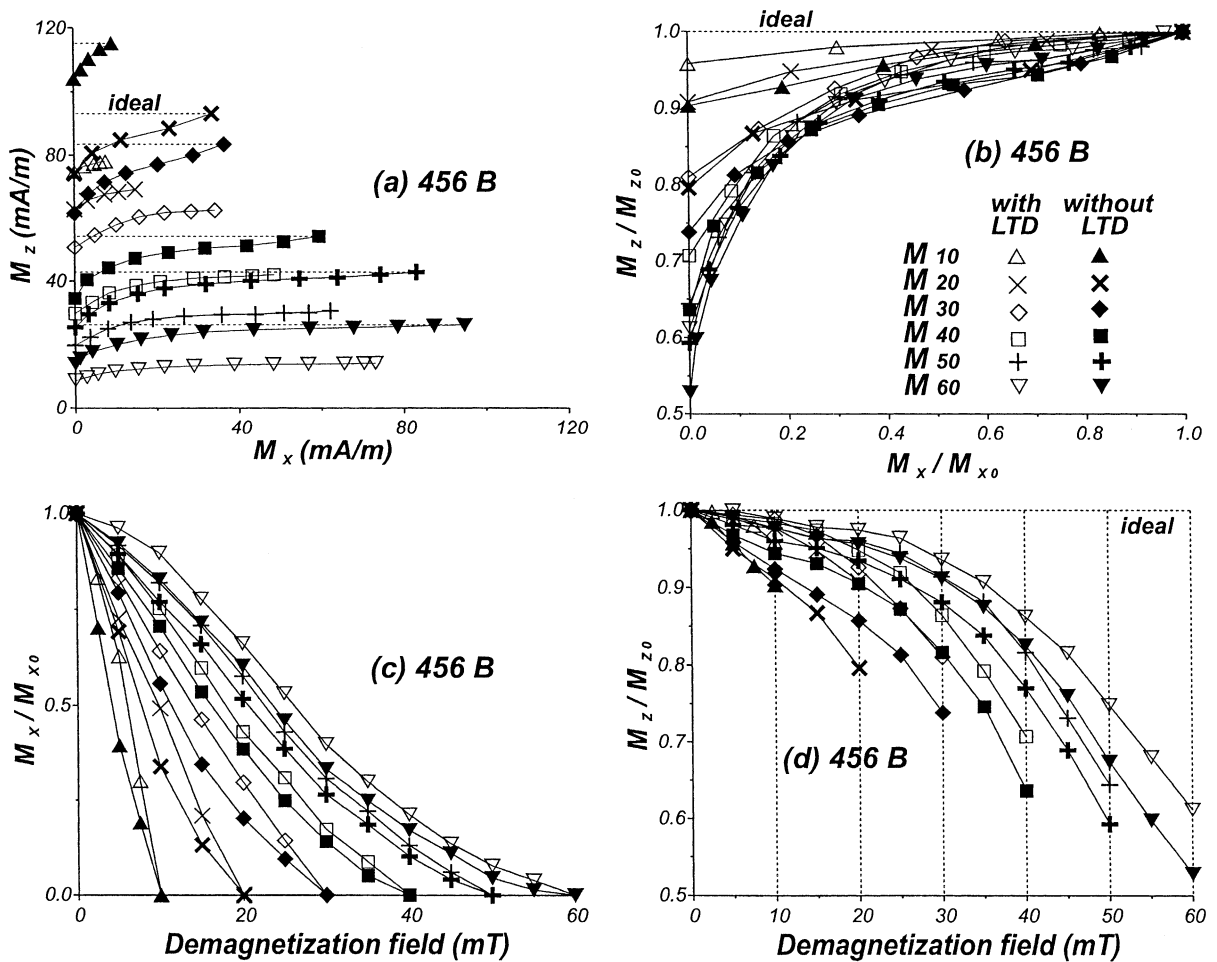


Fig. 7. AF demagnetization of  $ARM_z+pARM_x$  for lake sediment sample 456 B with and without LTD. (a) Vector plots. (b) Normalized vector plots. Decay curves for (c)  $x$  and (d)  $z$  components.

resents the degree of independence for each  $\tilde{H}_i$  (Fig. 5b; compare with the ideal trajectory which has an intercept  $M_z/M_{z0}=1$ ). Although not shown, the results for synthetic PSD samples are similar to the SD results.

The results for synthetic MD magnetite (16.9  $\mu\text{m}$ ) are interesting because LTD transforms an exponential decay of  $M_x$  into a more distributed decrease of remanence (Fig. 6c). However, LTD does not produce any SD-like initial plateaus, implying that LTD on MD grains is not as effective as on SD/PSD magnetites. The decay of  $M_z$  is striking (Fig. 6d) because the curves before and after LTD form two sets with distinct shapes. In

vector projections, continuous curved trajectories change their shapes to more orthogonal forms although the overprint field direction is still not perfectly recovered (Fig. 6a). In normalized vector plots, the improvement of independence is typically 5–10% (Fig. 6b).

Since ARM simulation has more relevance to the NRM of sediments than of igneous rocks, it is of special interest to examine lake sediments. Significant enhancement of SD-like stable remanence is visible both for  $x$  and  $z$  components in Fig. 7c,d. As a result, vector plots have better orthogonality after LTD (Fig. 7a,b). The improvement of independence is typically 5–11% (Fig. 7b).

### 4.3. Quantitative analyses

Figs. 5, 6, and 7 illustrate how LTD improves the independence of orthogonal remanences in AF demagnetization by making vector plots closer to the ideally orthogonal form and reducing the fraction of  $M_z$  that is demagnetized below  $\tilde{H}_i$ . In this section, two quantitative approaches will be used in order to assess the improvement after LTD.

In a paleomagnetic approach, since the  $z$  component  $M_z$  has unidirectional decay at AFs  $> \tilde{H}_i$ , we carried out principal component analysis (PCA) [24] on the portion with  $\tilde{H} < \tilde{H}_i$ , using standard software [25]. In the ideal situation of total independence, the inclination ( $I$ ) over AFs  $< \tilde{H}_i$  is  $0^\circ$  since  $M_z$  would remain constant while  $M_x$  is decaying. The results of this independence analysis for selected samples appear in Table 2. For synthetic SD (0.065  $\mu\text{m}$ ), PSD (0.24  $\mu\text{m}$ ), 456 B (lake sediment), and Km 3 (red scoria), it is quite clear that LTD shallows  $I$ , giving an improved estimate of the overprint direction, which is ideally  $I=0$ , as well as reducing the maximum angular deviation (MAD) [24], i.e., making the trajectories more linear. However, LTD gives no improvement for synthetic MD (16.9  $\mu\text{m}$ ), S 50 (granite), and T 2 (gabbro). In these samples, LTD neither shallows  $I$  nor reduces MAD. In fact, LTD increases MAD and  $I$  in most  $\tilde{H}_i$  intervals.

In vector plots, some of the results (Figs. 5, 6, and 7) show rather curved trajectories. Applying PCA to these portions is clearly an oversimplification. However, the relatively small values of MAD of  $< 10^\circ$  justify this approach in the context of this study.

For the second quantitative analysis, we used normalized vector plots. The value of the intercept (i.e.,  $M_z/M_{z0}$ ) on normalized vector plots is a measure of the degree of independence at each  $\tilde{H}_i$  (Figs. 5b, 6b, 7b, and Table 3). Ideally the intercept should be  $M_z/M_{z0} = 1$ . The measured values for the degree of independence are listed in Table 3. The violation of independence increases (values of  $M_z/M_{z0}$  or  $M_z/M_{z0}^{\text{LTD}}$  decreasing) as  $\tilde{H}_i$  increases (Table 3 and Fig. 8). The improvement in the degree of independence is significant (15–

Table 2  
Estimation of inclination and maximum angular deviation (MAD)<sup>a</sup>

Sample	$\tilde{H}$ (mT)	$n$	Without LTD		With LTD	
			MAD ( $^\circ$ )	$I$ ( $^\circ$ )	MAD ( $^\circ$ )	$I$ ( $^\circ$ )
Ideal			0.0	0.0	0.0	0.0
0.065 $\mu\text{m}$	10	5	9.8	27.6	3.2	18.1
	20	5	7.1	20.7	3.9	15.3
	30	7	6.7	22.2	2.5	16.0
	40	9	5.0	12.1	3.3	10.0
	50	11	2.5	5.6	1.9	4.6
	60	13	1.6	3.5	1.2	2.5
0.24 $\mu\text{m}$	10	5	6.8	65.8	2.7	31.3
	20	5	7.9	35.9	4.9	28.8
	30	7	6.6	21.6	3.5	21.1
	40	9	5.7	16.6	4.1	15.5
	50	11	3.9	11.7	3.0	10.0
	60	13	3.1	7.2	2.7	7.8
16.9 $\mu\text{m}$	10	5	4.0	16.7	3.1	12.2
	20	5	2.9	8.2	1.8	8.1
	30	7	3.0	6.5	3.6	8.7
	40	9	2.5	5.0	2.7	6.4
	50	11	1.1	2.3	1.4	3.7
	60	13	0.6	1.3	0.9	2.4
456 B	10	5	5.3	51.4	4.8	23.2
	20	5	6.5	27.1	6.2	22.5
	30	7	7.1	28.1	7.1	18.6
	40	9	6.9	15.1	6.0	12.4
	50	11	4.9	9.6	4.4	7.9
	60	13	3.4	6.0	1.9	3.4
Km 3	10	5	5.5	36.5	1.2	22.3
	20	5	7.2	23.5	2.9	28.3
	30	7	8.2	19.7	7.8	22.6
	40	9	7.7	14.9	5.7	13.9
	50	11	7.6	13.1	6.6	13.6
	60	13	5.7	9.2	5.4	10.0
T 2	10	5	10.9	27.7	8.4	24.4
	20	5	6.7	14.8	7.3	21.0
	30	7	6.3	14.2	9.2	17.0
	40	9	8.6	14.6	8.3	17.0
	50	11	8.6	13.3	7.9	15.7
	60	13	8.1	14.1	7.8	16.1
S 50	10	5	7.1	28.7	1.6	32.1
	20	5	4.4	15.7	4.8	21.3
	30	7	5.2	13.0	6.9	21.4
	40	9	5.5	12.1	6.2	16.4
	50	11	3.6	7.1	3.5	8.2
	60	13	4.1	7.7	3.4	8.6

<sup>a</sup>  $n$ : number of data points used in PCAs;  $\tilde{H}$ : peak AF of simulated remagnetization;  $I$ : inclination. Calculations were carried out using commonly used software [25].

20%) for synthetic MD (16.9  $\mu\text{m}$ ) and for S 50 (granite) but rather small (10% or less) for other samples.

Table 3  
Degree of independence<sup>a</sup>

Sample	$\tilde{H}_i$ (mT)	$M_z/M_{z0}$ <sup>LTD</sup>	$M_z/M_{z0}$	$M_z/M_{z0}$ <sup>LTD</sup> – $M_z/M_{z0}$ (%)
0.065 $\mu\text{m}$	10	0.971	0.932	3.9
	20	0.937	0.853	8.4
	30	0.810	0.656	15.4
	40	0.569	0.481	8.8
	50	0.461	0.354	10.7
	60	0.347	0.254	9.3
0.24 $\mu\text{m}$	10	0.943	0.818	12.5
	20	0.882	0.757	12.5
	30	0.762	0.643	11.9
	40	0.629	0.515	11.4
	50	0.490	0.371	11.9
	60	0.394	0.314	8.0
16.9 $\mu\text{m}$	10	0.932	0.746	18.6
	20	0.843	0.629	21.4
	30	0.694	0.416	27.8
	40	0.456	0.271	18.5
	50	0.365	0.126	23.9
	60	0.290	0.064	22.6
456 B	10	0.958	0.903	5.5
	20	0.908	0.796	11.2
	30	0.810	0.738	7.2
	40	0.707	0.626	8.1
	50	0.644	0.593	5.1
	60	0.612	0.528	8.4
Km 3	10	0.958	0.903	5.5
	20	0.908	0.796	11.2
	30	0.81	0.738	7.2
	40	0.707	0.636	7.1
	50	0.644	0.593	5.1
	60	0.612	0.528	8.4
T 2	10	0.930	0.872	5.8
	20	0.886	0.821	6.5
	30	0.826	0.767	5.9
	40	0.770	0.700	7.0
	50	0.691	0.608	8.3
	60	0.588	0.504	8.4
S 50	10	0.871	0.689	18.2
	20	0.712	0.546	16.6
	30	0.533	0.421	11.2
	40	0.471	0.338	13.3
	50	0.397	0.273	12.4
	60	0.318	0.211	10.7

<sup>a</sup>  $\tilde{H}_i$ : peak AF of simulated remagnetization.

## 5. Discussion

### 5.1. Low-temperature memory

Although many other studies have systematically investigated demagnetization of different remanences before and after LTD, either they were confined to narrow ranges of domain states of magnetites or they used AF demagnetization only [1,10,17,19,20,26]. In particular, thermal demagnetization of ARM memory has not previously been reported. Since most previous studies discussed detailed physical processes at low temperatures, the discussion in this section is confined to the new aspects only.

1. LTD improves SD-like features of the thermal demagnetization response of ARM, TRM, and SIRM dramatically. After LTD, the remanences show almost no decay from 20°C to 500–540°C and most unblocking temperatures ( $T_{\text{UBS}}$ ) are confined to a narrow interval from 500–540°C to 580°C. It is thus clear that LTD improves the stability of thermal demagnetization at the expense of fractions with  $T_{\text{UB}} < 500\text{--}540^\circ\text{C}$ . In thermal demagnetization of memories, it is unnecessary to have closely spaced steps up to 500–540°C. On the other hand, only a limited number of closely spaced high-temperature steps are possible in Thellier experiments on LTD-treated remanences. The situation is quite different in AF demagnetization of ARM, TRM, and SIRM memories. LTD affects broad coercivity intervals and will enhance pseudo-Thellier experiments by generating more uniformly spaced data points in an Arai plot.
2. During the AF demagnetization of samples containing SD/PSD magnetite (Fig. 2a,b,e), the curves for ARM, TRM, and their memories converge at intermediate AFs ( $\sim 25$  mT) and lie above the decay trend of SIRM or SIRM memory. On the other hand, for MD magnetite and granite S 50 (Fig. 2c,f), AF demagnetization curves of ARM, TRM, SIRM, and their memories all converge to a common trend (around 30 mT for synthetic MD grains and 10 mT for S 50).
3. Thermal demagnetization of ARM, TRM, and

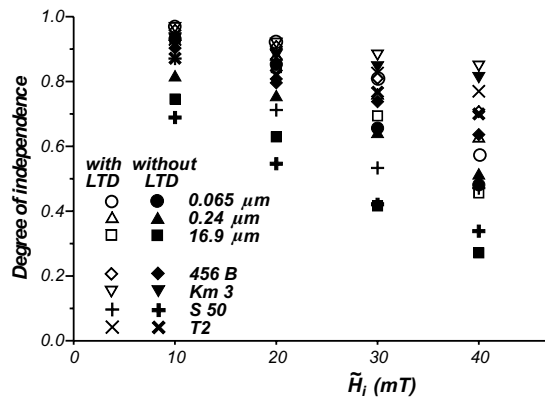


Fig. 8. Degree of independence  $M_z/M_{z0}$  or  $M_z/M_{z0}^{\text{LTD}}$  as a function of remagnetizing field  $\tilde{H}_i$ . The degree of independence decreases as  $\tilde{H}_i$  increases.

SIRM is a useful tool in identifying average grain size. For SD ( $0.065 \mu\text{m}$ ), ARM and TRM are more resistant to thermal demagnetization than SIRM. For PSD ( $0.24 \mu\text{m}$ ), the relative hardness of remanence is  $\text{TRM} > \text{ARM} > \text{IRM}$ . For MD ( $16.9 \mu\text{m}$ ), although the order of hardness is similar to that of SD, there is a distinct characteristic of distributed  $T_{\text{UBS}}$ . The different thermal stabilities of ARM and TRM are a hallmark of fine PSD magnetite [19,21,22]. However, this feature of fine PSD grains is diminished as a result of LTD (Fig. 2b,e).

4. Sample Km 3 shows interesting thermal behavior. Without LTD, TRM is the hardest and ARM is harder than SIRM, mimicking PSD characteristics of magnetite. After LTD, ARM, TRM, and SIRM memories still preserve relatively soft unblocking fractions, and decay similarly to untreated ARM, TRM, and SIRM, respectively. Interestingly, Km 3 had the most SD-like behavior among natural samples in terms of hysteresis ratio ( $M_{\text{rs}}/M_{\text{s}} = 0.40$ , Yu et al. [8], table 3). Since Km 3 contains titanomagnetite ( $x \approx 0.1$ , Yu et al. [8], table 3) rather than magnetite, it is clear that properties 1–3 must be confined to magnetite-bearing samples.

### 5.2. Can LTD improve the resolution of orthogonal pARMs?

The main goal in this study was to test whether

or not LTD improves the resolution of superimposed remanences in multivectorial directional analyses. Overall, LTD does improve the resolution of superimposed pARMs, but it is not a wholehearted success.

It is paleomagnetically interesting that estimated values of  $I$ , with or without LTD, deviate consistently from the ideal value of  $0^\circ$ . For most overprinting coercivities  $\tilde{H}_i < 40 \text{ mT}$ , no  $I$  is smaller than  $10^\circ$  (Table 2). Failure to estimate the correct direction of overprinting remanence is universal, regardless of grain size or lithology, except for the  $16.9 \mu\text{m}$  magnetite. This result has serious implications for paleomagnetic studies of multivectorial remanences. The ‘primary NRM’ direction would be perfectly recovered, but the overprint direction could be seriously in error.

According to analysis using normalized vector plots (Section 4.3), LTD-treated samples show universal improvement in the degree of independence of their  $x$ - and  $z$ -directional components, as measured by  $M_z/M_{z0}$ . Ideally  $M_z$  is not demagnetized at all for  $\tilde{H} < \tilde{H}_i$  ( $M_z/M_{z0} = 1$ ). The improvement is most significant (15–20%) for synthetic MD magnetite ( $16.9 \mu\text{m}$ ).

Component decay plots (Figs. 5c,d, 6c,d, 7c,d) and conventional vector plots (Figs. 5a, 6a, 7a) also indicate improved separation of  $x$ - and  $z$ -direction remanences after LTD. As a result, for most samples, inclinations of the remanence erased from 0 to  $\tilde{H}_i$  become shallower and closer to the ideal  $I = 0$ , while MAD values are reduced (Table 2). However, in the paleomagnetic ap-

proach, it is remarkable that the results without LTD actually give a closer estimate of the remagnetization field direction  $H_2$  for synthetic MD magnetite (16.9  $\mu\text{m}$ ), S 50 (granite), and T 2 (gabbro). In these samples, LTD actually increases inclination and MAD. This is puzzling since LTD shows signs of improving other aspects of independence (Figs. 2 and 6).

The MD characteristic of large amounts of AF demagnetization at low coercivity is responsible for this paradox. For example, for  $M_{30}$  of synthetic MD magnetite, AF demagnetization without LTD shows a drastic decrease of  $M_x$  between 0 (130.3 mA/m) and 15 mT (20 mA/m). These are the remanence fractions that dominate the  $I$  calculation, although statistical analysis uses the whole overprinting fraction ( $\tilde{H}_i, 0$ ). On the other hand, for  $M_{30}^{\text{LTD}}$  of synthetic MD magnetite, the decay of  $M_x$  is distributed more evenly so that the  $I$  calculation relies on the whole fraction.

One must also be cautious in using normalized vector plots. These can be useful in comparing data from different samples or from different  $\tilde{H}_i$  values for the same sample. On the other hand, normalized vector plots misrepresent the data in the sense that each set of data is normalized by quite different  $M_x$  and  $M_z$  intensities. For example, intensities of  $M_{x(10\text{ mT})}$ ,  $M_{x(10\text{ mT})}^{\text{LTD}}$ ,  $M_{z(10\text{ mT})}$ ,  $M_{z(10\text{ mT})}^{\text{LTD}}$ ,  $M_{x(30\text{ mT})}$ ,  $M_{x(30\text{ mT})}^{\text{LTD}}$ ,  $M_{z(30\text{ mT})}$ , and  $M_{z(30\text{ mT})}^{\text{LTD}}$  for 16.9  $\mu\text{m}$  are 66.7, 12.8, 85.3, 40.3, 130.3, 33.9, 28.5, and 18.3 mA/m, respectively (Fig. 6). Apparent improvement of independence judged from  $M_z/M_{z0}$  on normalized vector plots or increase of AF stability cannot necessarily guarantee a better resolution of multivectorial NRM using standard paleomagnetic analysis techniques, such as PCA.

## 6. Conclusion

Overall, LTD usually leads to a better resolution of component vectors and their directions in multivectorial sums. However, applying LTD requires careful prior study before use in each individual case since enhancement of SD-like behavior in normalized vector plots or AF demagnetization of separated components does not

necessarily guarantee success in resolving paleomagnetic component vectors by standard techniques such as PCA of linear segments on (unnormalized) orthogonal vector plots.

## Acknowledgements

Stefanie Brachfeld generously donated a large collection of lake sediment samples for use in this study. We thank Mike Jackson and Peat Solheid of the Institute of Rock Magnetism (IRM) for their help with the MPMS measurements. The Keck Foundation, the Earth Sciences Division of the National Science Foundation, and the University of Minnesota provide funding for the IRM. Helpful reviews by Phillip Schmidt and an anonymous referee improved the paper. This research has been supported by the Natural Sciences and Engineering Research Council of Canada through Grant A7709 to D.J.D. [RV]

## References

- [1] M. Ozima, M. Ozima, S. Akimoto, Low temperature characteristics of remanent magnetization of magnetite, *J. Geomagn. Geoelectr.* 16 (1964) 165–177.
- [2] P.W. Schmidt, Paleomagnetic cleaning strategies, *Phys. Earth Planet. Inter.* 76 (1993) 169–178.
- [3] D.J. Dunlop, P.W. Schmidt, Ö. Özdemir, D.A. Clark, Paleomagnetism and paleothermometry of the Sydney Basin: 1. Thermoviscous and chemical overprinting of the Milton Monzonite, *J. Geophys. Res.* 102 (1997) 27271–27284.
- [4] D.J. Dunlop, Ö. Özdemir, P.W. Schmidt, Paleomagnetism and paleothermometry of the Sydney basin 2. Origin of anomalously high unblocking temperatures, *J. Geophys. Res.* 102 (1997) 27285–27295.
- [5] A.C. Warnock, K.P. Kodama, P.K. Zeitler, Using thermochronometry and low-temperature demagnetization to accurately date Precambrian paleomagnetic poles, *J. Geophys. Res.* 105 (2000) 19435–19453.
- [6] G.J. Borradaile, F. Lagroix, D. Trimble, Improved isolation of archeomagnetic signals by combined low temperature and alternating field demagnetization, *Geophys. J. Int.* 147 (2001) 176–182.
- [7] Y. Yu, D.J. Dunlop, Ö. Özdemir, Testing the independence law of partial ARMs: implications for paleointensity determination, *Earth Planet. Sci. Lett.* (2002) S0012-821X(02)01150-0.
- [8] Y. Yu, D.J. Dunlop, Ö. Özdemir, Partial anhysteretic

- remanent magnetization in magnetite 1. Additivity, *J. Geophys. Res.* 107 (B10) (2002) 10.1029/2001JB001249.
- [9] Y. Yu, D.J. Dunlop, Ö. Özdemir, Partial anhysteretic remanent magnetization in magnetite 2. Reciprocity, *J. Geophys. Res.* 107 (B10) (2002) 10.1029/2001JB001269.
- [10] A.R. Muxworthy, E. McClelland, The causes of low-temperature demagnetization of remanence in multidomain magnetite, *Geophys. J. Int.* 140 (2000) 115–131.
- [11] Y. Yu, Rock Magnetic and Paleomagnetic Experiments on Hemoilmenites and Titanomagnetites in Some Volcanic Rocks from Japan, M.Sc. Thesis, University of Toronto, Toronto, ON, 1998, 24 pp.
- [12] Y. Yu, D.J. Dunlop, Paleointensity determination on the late Precambrian Tudor Gabbro, Ontario, *J. Geophys. Res.* 106 (2001) 26331–26344.
- [13] Y. Yu, D.J. Dunlop, Multivectorial paleointensity determination from the Cordova Gabbro, southern Ontario, *Earth Planet. Sci. Lett.* 203 (2002) 983–998.
- [14] D.J. Dunlop, Paleomagnetism of Archean rocks from northwestern Ontario: 4. Burchell Lake granite, Wawa-Shebandowan Subprovince, *Can. J. Earth Sci.* 21 (1984) 1098–1104.
- [15] D.J. Dunlop, L.D. Schutts, C.J. Hale, Paleomagnetism of Archean rocks from northwestern Ontario: 3. Rock magnetism of the Shelley Lake granite, Quetico Subprovince, *Can. J. Earth Sci.* 21 (1984) 879–886.
- [16] S.A. Brachfeld, S.K. Banerjee, A new high-resolution geomagnetic relative paleointensity record for the North American Holocene: A comparison of sedimentary and absolute intensity data, *J. Geophys. Res.* 105 (2000) 821–834.
- [17] F. Heider, D.J. Dunlop, H.C. Soffel, Low-temperature and alternating field demagnetization of saturation remanence and thermoremanence in magnetite grains, *J. Geophys. Res.* 97 (1992) 9371–9381.
- [18] D.J. Dunlop, Ö. Özdemir, *Rock Magnetism: Fundamentals and Frontiers*, Cambridge University Press, New York, 1997, 573 pp.
- [19] D.J. Dunlop, K.S. Argyle, Separating multidomain and single-domain-like remanences in pseudo-single-domain magnetites (215–540 nm) by low-temperature demagnetization, *J. Geophys. Res.* 96 (1991) 2007–2017.
- [20] Ö. Özdemir, D.J. Dunlop, Single-domain-like behavior in a 3 mm natural single crystal of magnetite, *J. Geophys. Res.* 103 (1998) 2549–2562.
- [21] D.J. Dunlop, G.F. West, An experimental evaluation of single domain theories, *Rev. Geophys.* 7 (1969) 709–757.
- [22] Y. Yu, D.J. Dunlop, Ö. Özdemir, Are ARM and TRM analogs?, Thellier analysis of ARM and pseudo-Thellier analysis of TRM, *Earth Planet. Sci. Lett.* 205 (2002) 325–336.
- [23] Ö. Özdemir, D.J. Dunlop, B. Moskowitz, Changes in remanence, coercivity, and domain state at low temperature in magnetite, *Earth Planet. Sci. Lett.* 194 (2002) 343–385.
- [24] J.L. Kirschvink, The least-squares line and plane and the analysis of paleomagnetic data, *Geophys. J. R. Astron. Soc.* 62 (1980) 699–718.
- [25] L. Tauxe, *Paleomagnetic Principles and Practice*, Kluwer Academic, Boston, MA, 1998, 299 pp.
- [26] V.V. Shcherbakova, V.A. Shcherbakov, P.W. Schmidt, M. Prévot, On the effect of low-temperature demagnetization of TRMs and pTRMs, *Geophys. J. Int.* 127 (1996) 379–386.